

Date of publication xxxx 00, 0000, date of current version xxxx 00, 0000.

Digital Object Identifier 10.1109/ACCESS.2017.Doi Number

An Improved Cuckoo Search Algorithm of Boundary Search and Variable Step-size For Gravitational Reference Sensor Parameters Identification

DEQUAN LI¹, HONGDA LIU^{1,2}, DONG WANG¹, ZHI WANG¹, AND XINGGUO SUN³

¹ Space Optics Department, Changchun Institute of Optics, Fine Mechanics and Physics, Chinese Academy of Sciences, Changchun, Jilin 130033, China

² University of Chinese Academy of Sciences, Beijing 100049, China

³ FAW-Volkswagen Automobile Co., Ltd

Corresponding author: Dong Wang (e-mail: wangd@ciomp.ac.cn) and Zhi Wang (wz070611@126.com)

This work was supported in part by the "Strategic Priority Research Program of the Chinese Academy of Science" (XDA1502070404)

ABSTRACT At this stage, in order to ensure the effective work of the gravitational reference sensor, it's necessary to ensure the residual velocity of the test mass (mass=1.9 kg) after being released by the grabbing positioning and release mechanism is less than 5 μ m/s, so that it can be normally captured by the electrode housing. Therefore, based on mathematical model of the release mechanism electro-mechanical dynamics, this paper conducts related research on the relationship between the residual speed of the test mass and the system parameters of the grabbing positioning and release mechanism. In order to solve the problem of difficulty in identifying model parameters, this paper uses the cuckoo search algorithm to identify model parameters, and improves the search efficiency and success rate by improving the step-length control factor and search strategy. Simulation experiments show that under the same number of iterations, the improved algorithm has achieved an effective improvement in the identification success rate and convergence accuracy of the original algorithm. Through the identification results, the residual speed of the test mass can be derived, verify whether the designed system meets the requirements, and establish an evaluation and guidance system for the system design.

INDEX TERMS Gravitational reference sensor, Grabbing positioning and release mechanism, Residual velocity, Cuckoo search algorithm, Parameter identification.

I. INTRODUCTION

The Laser Interferometer Gravitational Wave Observatory (LIGO) in the United States detected the first gravitational wave signal on September 14, 2015 [1]. In addition to the United States, many countries are also actively constructing ground-based gravitational wave observatories, such as VIRGO in Italy, GEO600 in Germany, and KaGRA in Japan. The space gravitational wave detection plan was first proposed by the United States. With the support of the European Space Agency (ESA), the Laser Interferometer Space Antenna (LISA) plan was finally formulated in 1997 [2]. Due to funding reasons, NASA withdrew from the LISA project in 2011 and was taken over by ESA. China has also formulated three space exploration plans: the Tianqin Project, the Ali Experiment Project, and the Taiji Project. "Tai Chi 1"

was successfully launched at the end of August 2019 and successfully completed the first phase of the on-orbit test mission. In 2020, the Chinese Academy of Sciences announced the launch of the space gravitational wave detection program-" Tai Chi 2" double star .

The principle of space gravitational wave detection is realized by the principle of laser interferometry. As the reference datum of the laser interferometric distance measurement system, the gravitational reference sensor is one of the most important parts of the space gravitational wave detection device [3]. One of its main functions is to use the grabbing positioning and release mechanism ensures that the test mass is safely and reliably fixed in the electrode cage during the launch phase. After the satellite enters orbit, the release mechanism is used to release the test mass (mass=1.9

kg) into the space at a residual velocity of less than $5\mu\text{m/s}$, and the electrostatic control system will control it. The residual speed of the test mass is related to the parameters of the release mechanism. If the speed is too high, the detection plan will fail. Therefore, the system design of the release mechanism is very important, which requires the establishment of the relationship between the system parameters of the release mechanism and the residual speed [4]. In this paper, the system parameters are identified through the simulation experiment data, and the residual velocity is derived. The results are used to guide the improvement and design of the grabbing positioning and release mechanism.

The parameters identification of the grabbing positioning and release mechanism will eventually transform the multi-parameter nonlinear optimization problem, so it is necessary to introduce an optimization algorithm to solve this problem. Yang and Deb of Cambridge University proposed Cuckoo Search (CS) in 2009 [5-6], which is an optimized algorithm designed by simulating the behavior of cuckoos seeking nests and laying eggs. The algorithm is simple, has few parameters, and is easy to implement. Researchers have applied it to solve many engineering optimization problems and obtained promising results [7-10]. Therefore, this paper uses this algorithm to identify the parameters of mathematical model of the release mechanism electro-mechanical dynamics. At the same time, this paper proposes an improved cuckoo search algorithm for the parameters identification from the following two aspects: (i) Improving the step-length control factor of the CS algorithm based on the population distribution entropy, which speeds up the identification of model parameters. (ii) Improving the local search strategy of the CS algorithm based on the boundary search strategy, which increases the success rate of the identification of model parameters.

II. FORMULATION OF MATHEMATICAL MODEL OF THE RELEASE MECHANISM ELECTRONIC MECHANICAL DYNAMICS

Cage and Vent Mechanism (CVM) is one of the core equipment of gravitational reference sensor, the main task of it is to maintain the position of the TM during the launch and release the TM at a low speed after reaching the designated orbit. CVM is composed of two parts located above and below TM. Each part contains two independent mechanisms, namely caging mechanism sub-system (CMSS) and grabbing positioning and release mechanism (GPRM). The upper and lower CMSS are responsible for locking the TM during the launch process. The CMSS in each part uses 4 actuators to drive 4 locking fingers to ensure that the TM is confined within the electrode housing (EH) before entering the designated orbit, preventing the TM from contacting the EH [11-13]. Once in the designated orbit, TM will be handed over to GPRM. GPRM works simultaneously with the release of CMSS. GPRM is mainly divided into an actuator

unit containing piezoelectric actuators and Grabbing Fingers (GF). GPRM will control the TM to move to the center of the EH and correct the TM's posture. Finally, the coaxial Release Tip (RT) in the GF moves toward the TM and contacts the TM, so that the GF can leave the TM [14-16]. However, when RT and TM are in contact, the surfaces of the two will have adhesion. GF quickly retracts RT through the internal piezoelectric laminated actuator, and uses the inertia of TM to achieve the failure of the adhesion between the two. Separate TM dynamically, and finally complete the release process of TM [17-20]. In order to mathematically describe the behavior of the TM during the inflight release phase, the following three models will be combined.

A. GPRM model

The release function of GPRM is performed by RT. The design purpose of RT is to minimize the contact area between GF and TM, thereby minimizing the residual speed caused by the adhesion force generated by the contact part. The simplified equations governing the piezo-actuator and RT are shown in equation (1) and equation (2) [3], the meaning of the symbols in the formulas is shown in Table 1.

$$RC\ddot{x}(t) + q(t) - T_p x_{RT}(t) = CE(t) \quad (1)$$

$$m\ddot{x}_{RT}(t) + b\dot{x}_{RT}(t) + (k + \frac{T_p^2}{C})x_{RT}(t) - \frac{T_p}{C}q(t) = 0 \quad (2)$$

TABLE 1
THE MEANING OF THE SYMBOLS IN THE FORMULA

Symbol	The meaning
$E(t)$	Input voltage
$q(t)$	Charge accumulated on the piezo
$x_{RT}(t)$	The resulting RT position
R	Resistance of the electrical circuit
C	Capacitance of the piezo-stack
T_p	Electromechanical transducer
m	Mass of the RT and half piezo-stack
b	Damping (result of the washer spring and piezo elasticity combined effect)
k	Stiffness (result of the washer spring and piezo elasticity combined effect)

The schematic structure of the GPRM is shown as Fig. 1. m_p , b_p , k_p are the mass, equivalent damping, equivalent stiffness of the piezoelectric element, b_{water} , k_{water} are the damping, stiffness result of the piezo elasticity, and F_p is the piezoelectric-generated force exerted by the stack on the environment, V_p is the voltage applied to the piezoelectric element, m_{RT} is the mass of the RT. x is deformation of piezoelectric element, q_p is the electric charge generated by the piezoelectric effect.

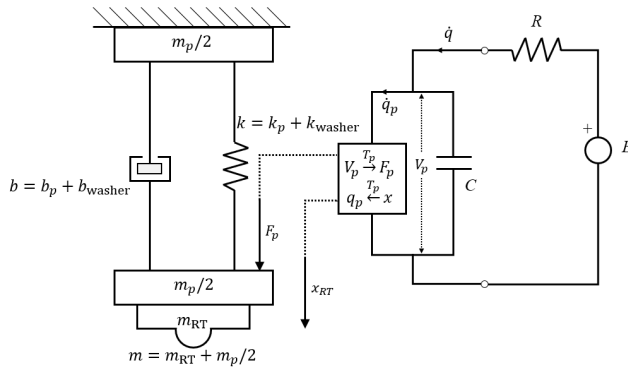


FIGURE 1. Lumped-element diagram of the GPRM.

The transfer function $G(s)$ of the displacement of RT with respect to the input E can be derived from equations (3), (4), (5), (6) and (7).

$$G(s) = \frac{X_{RT}(s)}{E(s)} = \frac{b_0}{a_3 s^3 + a_2 s^2 + a_1 s + 1} \quad (3)$$

$$b_0 = \frac{T_p}{k} \quad (4)$$

$$a_3 = \frac{mRC}{k} \quad (5)$$

$$a_2 = \frac{bRC + m}{k} \quad (6)$$

$$a_1 = RC + \frac{RT_p^2}{k} + \frac{b}{k} \quad (7)$$

When the TM is driven to the target position, the RT will be de-energized and contracted. However, the input voltage $E(t)$ can not be measured because the power-off speed time is too short. In order to facilitate the study of the relationship between the residual speed and system parameters, this paper uses an ideal step voltage from 0V to 120V as the system input. Therefore, the displacement expression of RT can be simplified to:

$$x_{RT}(s) = \frac{b_0}{a_3 s^3 + a_2 s^2 + a_1 s + 1} * \frac{120}{s} \quad (8)$$

The time domain expression of RT displacement is shown:

$$x_{RT}(t) = \mathbf{I}^{-1}[x_{RT}(s)] = \mathbf{I}^{-1} \left[\frac{b_0}{a_3 s^3 + a_2 s^2 + a_1 s + 1} * \frac{120}{s} \right] \quad (9)$$

B. Adhesion force model

Scholars from the University of Trento have developed a device specifically used to test adhesion under the approximate conditions of LPF, called the Transferred Momentum Measurement Facility (TMMF) [3]. The TMMF can measure the residual velocity of the suspended TM after the RT is quickly retracted. The model of TM and RT is used to estimate the adhesion force model included in the overall

mathematical model of the TM during the predetermined orbital release process to predict the release speed.

In TMMF, the acceleration of TM reflects the size of the adhesion force. The adhesion force is related to the relative distance between RT and TM. The dynamic behavior of the adhesion between the two can be regarded as a function of the relative distance between the two, where the movement of RT is regarded as the input of the system, and the movement of TM is regarded as the output of the system. The exponential function has been used to describe the adhesion of the stretch profile, here the equation (10) is used [3], $E(t)$ is the elongation, X_1 and X_2 and X_3 are the parameters to be estimated. The exponential function is chosen mainly because the model curve matches the observed system behavior empirically, and it is easier to implement it with exponential function approximation. This article is based on [3] to construct the adhesion model and parameters used are also the same as in the reference [3].

$$F_{adh}(Dl) = X_1 D l e^{-X_2 D l^{X_3}} \quad (10)$$

C. Residual velocity model of TM

In the case of single-sided release [3], the single-sided adhesion is the only external force that TM receives, the size of the adhesion reflects the acceleration of TM, as shown in Fig. 2. From equation (1) and equation (2), the joint model of GPRM and TM can be obtained as equation (11). The adhesion force is introduced in equation (12), but because the value of the adhesion force is small relative to the forces of other terms, the influence of the adhesion force is negligible. Using Runge-Kutta algorithm to calculate X_{TM} numerically by equations (11), (12) and (13), the residual velocity of TM can be obtained.

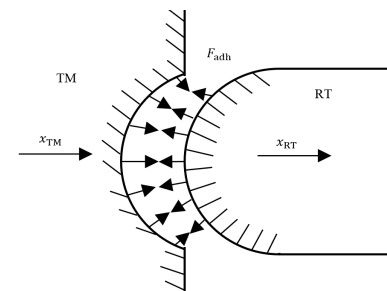


FIGURE 2. Schematic diagram of TM force when released on one side.

$$RC \ddot{x}(t) + q(t) - T_p x_{RT}(t) = CE(t) \quad (11)$$

$$m \ddot{x}_{RT}(t) + b \dot{x}_{RT}(t) + \left(k + \frac{T_p^2}{C}\right) x_{RT}(t) - \frac{T_p}{C} q(t) + \quad (12)$$

$$X_1 (x_{RT}(t) - x_{TM}(t)) e^{-X_2 (x_{RT}(t) - x_{TM}(t))^{X_3}} = 0$$

$$M \ddot{x}_{TM}(t) - X_1 (x_{RT}(t) - x_{TM}(t)) e^{-X_2 (x_{RT}(t) - x_{TM}(t))^{X_3}} = 0 \quad (13)$$

In this paper, the RT displacement curve is mainly used to identify the relevant parameters of the grabbing positioning and release mechanism. After the identification, it is combined with the known adhesion force model to calculate the residual velocity of the test mass.

The objective function of RT displacement curve parameter identification is the root mean square error (RMSE) between the RT displacement curve calculated by the model after parameter identification and the RT experimental displacement curve:

$$RMSE = \left(\frac{\sum_{n=1}^N (x_{RT}(n, a_3^r, a_2^r, a_1^r, b_0^r) - x_{RT}(n))^2}{N} \right)^{1/2} \quad (14)$$

$x_{RT}(t)$ is the sampling point at time n of RT displacement curve, $a_3^r, a_2^r, a_1^r, b_0^r$ are the parameters identified by the optimization algorithm.

III. IMPROVED CUCKOO SEARCH ALGORITHM

With the development of science and technology, optimization problems have become the key research objects in various fields. Some optimization algorithms are popular due to their advantages such as simple algorithm and easy implementation [21-24], especially the cuckoo search algorithm proposed by Yang and Deb of Cambridge University in 2009. This is an optimization algorithm designed by simulating the behavior of cuckoos looking for nests and laying eggs. It is optimized based on the Levy flight mechanism, which can effectively solve the optimization problem and has been successfully applied to image processing, system design, medical applications, data mining and other fields, this paper will use this algorithm to identify the parameters of the grabbing positioning and release mechanism.

A. Cuckoo search algorithm

Cuckoo Search (CS) uses Levy Flight to effectively solve the optimization problem by simulating the principle of cuckoo nest parasitic reproduction. The algorithm is based on three ideal conditions:

- (1) The cuckoo lays only one egg at a time, and randomly selects the host bird nest to hatch its own eggs;
- (2) In a randomly selected set of bird nests, the bird nest with the best hatching conditions will be retained for the next generation;
- (3) The number of host bird nests N is fixed, and the probability of the parasitic eggs being found is $p_a \in [0, 1]$.

On the basis of the above three ideal conditions, CS searches for the bird's nest path and location update formula according to the Levy flight model simulated based on the Mantegna method as follows:

$$z^{k+1} = z^k + a \left(z^k - z_{best} \right) \text{Levy}(l) \quad (15)$$

$$\text{Levy}(l) = m / |l|^{1/b} \quad (16)$$

z^{k+1} and z^k are the host nest positions of the $k+1$ and k generations, z_{best} is the current optimal solution, a is the step-length control factor, and $\text{Levy}(\lambda)$ is the Levy flight formula, $b = 1.5$, $m: N(0, s_m^2)$, $v: N(0, 1)$. Standard deviation s_m of normal distribution can be calculated according to equation (17).

$$s_m = \frac{\Gamma(1+b) * \sin(\pi b / 2)}{\Gamma(b) * \Gamma(b-1/2)} * \frac{1}{b} \quad (17)$$

p_a is the probability of the parasitic egg being found, generally $p_a = 0.25$. After the CS algorithm updates the position through the Levy flight, it generates a random number r . When $r > p_a$, it uses a random walk method for z^k to generate an equal amount of new solutions to replace the old solutions, which symbolizes the discovery of the parasitic egg, the cuckoo randomly selects a new nest for parasitic reproduction. The random walk formula is shown in equation (18), the compression factor $h = U[0, 1]$, z_a^k and z_b^k represent two random solutions of the k -th generation.

$$z^{k+1} = z^k + h \left(z_a^k - z_b^k \right) \quad (18)$$

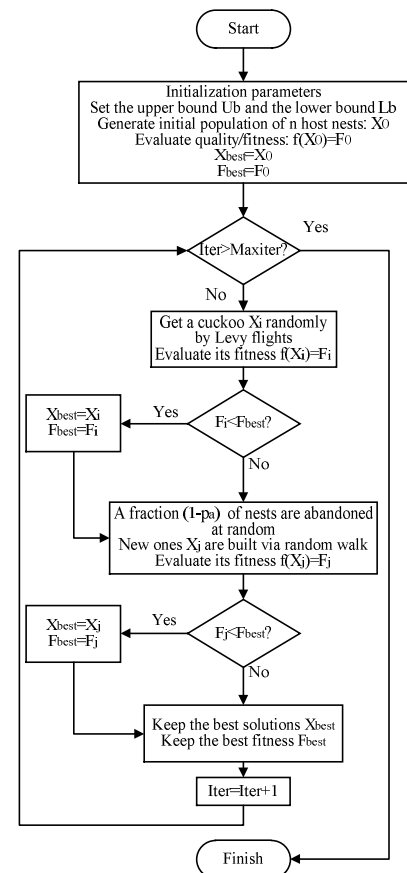


FIGURE 3. The flow chart of CS algorithm.

When dealing with actual optimization problems, the position of the bird's nest represents the solution value of the variable to be identified, and the fitness of the bird's nest represents the value of the corresponding objective function when the variable to be identified takes different solutions. The algorithm flow chart is shown as in Fig. 3.

B. Improved cuckoo search algorithm

1) IMPROVEMENT OF STEP CONTROL FACTOR BASED ON POPULATION ENTROPY

From equations (15), (16) and (17), it can be seen that the value of Levy(λ) depends on the normally distributed random numbers m and v , which leads to highly random changes in Levy's flight search step length and direction. Therefore, the step size control factor a is very important. A larger control factor can enhance the global search ability, but the local search ability is poor, which is likely to cause the search to swing near the true value; a smaller control factor will lead to the inefficiency of the algorithm. In the cuckoo search algorithm, the step-length control factor a is constant, and the search performance of the algorithm cannot be used well. Therefore, this paper introduces the concept of population distribution entropy into the CS algorithm to improve the step length control factor.

Entropy is a measure of the confusion degree of a certain system, and population entropy [25-26] is a measure of the confusion degree of population distribution in the process of algorithm optimization. Assuming that the total number of cuckoo populations is N and the search dimension is dim , the optimization search space is divided into K search subspaces, and each subspace contains the number of individuals n_i ($i=1,2,\dots,K$), then the distribution entropy of the j -th dimension as shown in equation (19).

$$S_j = - \sum_{i=1}^K \frac{n_i}{N} \ln \frac{n_i}{N} \quad (19)$$

In order to make the distribution entropy better reflect the distribution information of the optimal solution, generally the search subspace K takes a large value. The larger the S , the more dispersed the population, which means that the algorithm does not converge, and a larger update step size is required for global search; the smaller S is, the more concentrated the population is, which indicates that the algorithm starts to converge, and a smaller update step size is required for local search. Therefore, the improved step length control factor is shown in formula equation (20).

$$a_j = q * \frac{S_j - S_{\min}}{S_{\max} - S_{\min}} \quad (20)$$

a_j is the step length control factor of the j -th dimension, $S_{\min} = 0$ is the theoretical minimum value of the distribution entropy, $S_{\max} = \ln K$ is the theoretical maximum value of the distribution entropy, and q is the adjustment parameter. Generally $K \gg N$, it can be seen in equation (19) that the

actual minimum value of the distributed entropy is 0, and the actual maximum value shown in formula equation (21).

$$S_{\max} = - N * \frac{1}{N} \ln \frac{1}{N} = (K - N) * 0 = \ln N \quad (21)$$

The value range of the step control factor is a $\hat{a} [0, q(\ln N / \ln K)]$. In this article $q = \ln K / \ln N$, so the value range of the step control factor is $[0, 1]$. However, when all the populations are gathered in the same area, the distribution entropy will be zero ($S = 0$) and cause the algorithm to no longer be updated. In this situation the step length control factor a is set $1 / K$ when $S = 0$.

2) IMPROVEMENT OF BOUNDARY SEARCH STRATEGY

In the process of using the CS algorithm to identify the parameters of the GPRM model, the coefficient of the transfer function will appear to be 0, but the six parameters are all effective physical quantities, and it is impossible to be equal to zero. Through analysis, it is found that when the true value is very close to the boundary value the CS algorithm will limit the optimization results, and the algorithm has a large initial update step, the boundary value will be regarded as the optimal search result. In this situation, the probability that the algorithm finds the true value is low, which makes the algorithm invalid.

In order to solve this problem, this paper introduces a local search jump-out mechanism to the CS. When the parameter to be identified in a certain dimension always takes the boundary value X_{bound} during the optimization process and does not change within a certain number of iterations. Taking multiple small values D of different magnitudes, add and subtract them to the boundary value in a certain dimension to generate a new value $X_{bound} + D$ and calculate the corresponding fitness $f(X_{bound} + D)$, and select the optimal fitness and the optimal magnitude of the value $X_{bound} + D$. If the fitness of the new value is better, it means that the true value of the parameter is closer to the new value, and the new value is replaced with the boundary value and the optimization is continued. The schematic diagram is shown in Fig. 4.

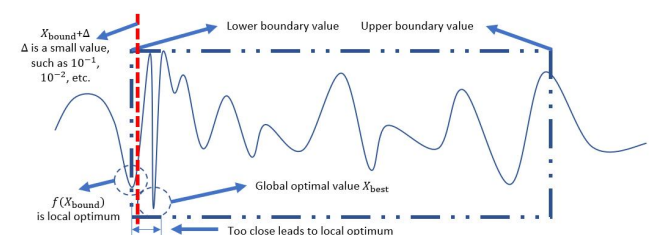


FIGURE 4. The schematic diagram of improvement mechanism.

C. Boundary search and variable step-size cuckoo search

The improved cuckoo search algorithm of boundary search is called boundary search cuckoo search (BSCS). The CS algorithm after the above two improvements is called

boundary search and variable step-size cuckoo search (BS-VSCS), the algorithm flowchart is shown as in Fig. 5.

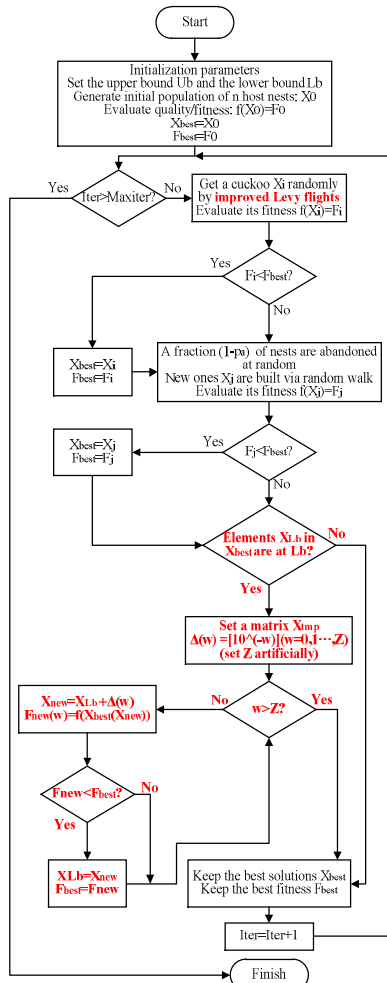


FIGURE 5. The flow chart of BS-VSCS algorithm.

IV. SIMULATION EXPERIMENT

A. Parameters identification of the RT displacement curves

The system parameters of the grabbing positioning and release mechanism in this paper are the same as those in [3]. The experimental test displacement curve of RT is shown in Fig. 5. , w represents the total magnitude changes of small value D , and Z is the current magnitude changes of small value D . X_{Lb} represents the lower bound value is the element in the matrix X_{best} .

It can be seen from Fig. 6 that the displacement of RT is on the order of microns and the time is on the order of milliseconds. If the standard unit is used for system identification, the identification coefficient will be too small which will affect the identification accuracy. If the physical meaning of the transfer function has not changed, the equivalent change of the unit of the system parameter can facilitate the identification of the parameter. After the

identification result is obtained, it can be restored to the standard unit or the corresponding equivalent unit according to the unit equivalence relationship. The changed parameter units are shown in Table 2.

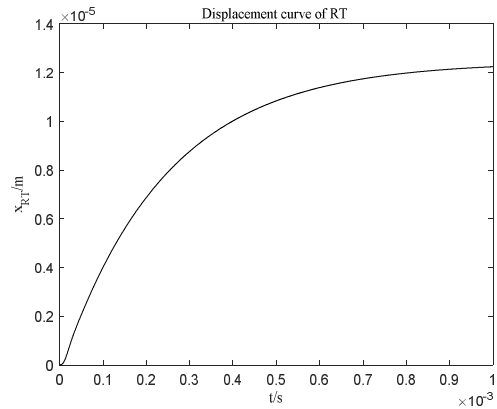


FIGURE 6. The displacement curve of RT.

TABLE 2
THE EQUIVALENCE BETWEEN OPTIMIZED UNIT AND STANDARD UNIT

Parameter	SI or derived units	Equivalent unit
R	Ω	0.001 k Ω
C	F	$10^6 \mu\text{F}$
T_p	$(\text{F} \cdot \text{N}/\text{m})^{1/2}$	$(\mu\text{F} \cdot \text{kg}/\text{ms}^2)^{1/2}$
k	N/m	$10^{-6} \text{kg}/\text{ms}^2$
b	$\text{N} \cdot \text{s}/\text{m}$	$10^{-3} \text{kg}/\text{ms}$
m	kg	kg
X_{RT}	M	$10^6 \mu\text{m}$
t	s	1000ms

The following identification true values of equation (10) and Fig. 6 which can be calculated using the relevant parameter values in the [3].

TABLE 3
THE IDENTIFICATION TRUE VALUES OF THE MODEL

Parameter	SI or derived units
b0	0.103630
a3	0.00000920651
a2	0.00163218
a1	0.247147

In this section, this article randomly generates 100 sets of data in the neighborhood of the true value of Table 3 to generate 100 sets RT displacement curves similar to Fig. 6. Respectively use the CS algorithm and the improved CS algorithm to identify the parameters of the RT displacement curves. The root mean square error between the displacement curve with the identification values and the displacement curve with the true values is used as the evaluation function, the populations of the two algorithms are 25, the search interval is divided into 10000, and the number of iterations is 400[10].

Fig.7 shows the results of 100 sets of simulation experiment data. The RMSE value is greater than 10^{-6} will

be regarded as identification failure. It can be seen from the Fig. 7a that the success rate of the CS algorithm in 100 optimizations is 84%, while the success rate of the BSCS algorithm is close to 100%. This is because in the optimization process of the CS algorithm, the true value of a certain dimension is closer to the lower boundary, which causes the CS algorithm to fall into a local optimal value within a limited number of optimization times, and the search fails. The improved BSCS avoids the occurrence of this phenomenon.

In addition, it can be seen from the Fig. 7b that under the same number of iterations, the average convergence accuracy of the BS-VSCS algorithm is 10^{-11} orders of magnitude, which is much higher than the 10^{-8} accuracy of the BSCS algorithm. The search accuracy of the BS-VSCS algorithm is much higher than that of the BSCS algorithm.

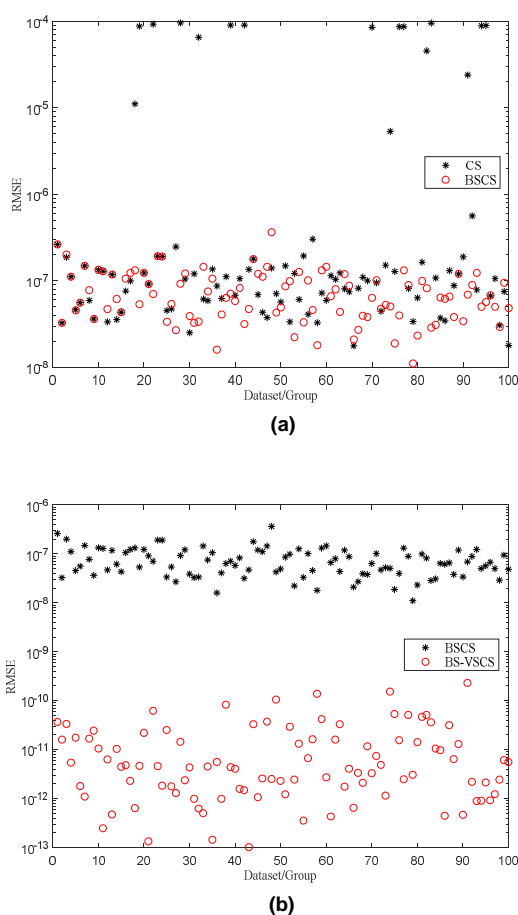


FIGURE 7. The optimization results of 100 different datasets. (a) BSCS VS CS. (b) BS-VSCS VS BSCS.

Fig. 8 shows the variation of RMSE with the number of iterations of different algorithms in a typical search process. It can be seen that the introduction of the local search jump-out mechanism can increase the success rate of algorithm optimization, and the improvement of the step size control factor can significantly increase the search accuracy of the algorithm.

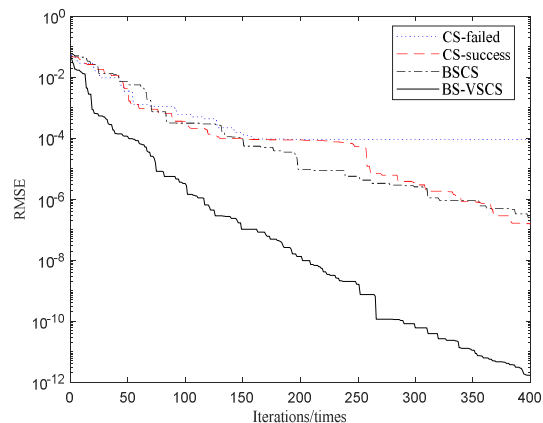


FIGURE 8. The displacement curve of RT. The RMSE the number of iterations under different algorithms.

Fig. 9 shows the change of the step size control factors of each dimension of BS-VSCS with the number of iterations during an algorithm optimization process. It can be seen that the step size control factors of each dimension change continuously with the population distribution entropy, and the overall trend is decreasing. As the number of iterations increases, the algorithm gradually shifts from global search to local search.

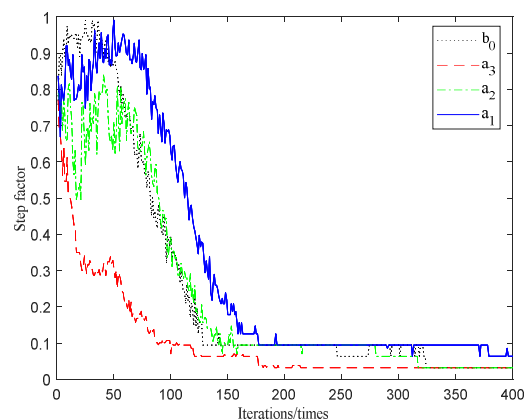


FIGURE 9. The variation curve of step factor with iterations

The above simulation experiment results prove the effectiveness of the improvement of the BS-VSCS algorithm in terms of step factor and search strategy.

Compared to other optimization algorithms, the CS algorithm is simple, has few parameters, and is easy to implement. In addition, this paper improves the CS algorithm according to actual needs, so that it has a faster convergence speed and a higher success rate for gravitational reference sensor parameters identification. The improved variable step control factor based on population entropy makes the improved CS algorithm have stronger search intelligence and improved strategy based on local boundary search makes the improved CS algorithm have stronger boundary search capabilities, which are not available in other algorithms.

B. Calculation of residual speed of test mass

In the experiment, after identifying the RT displacement curve to obtain the identification result of the value of a_3 、 a_2 、 a_1 and b_0 . The value of T_p 、 k and b can be calculated by equations(4),(5),(6)and(7) and the prior values of R, C, and M. Thus, the relationship between the parameters of the grabbing positioning and release mechanism and the residual speed of the test mass can be established by equations (11),(12) and(13).

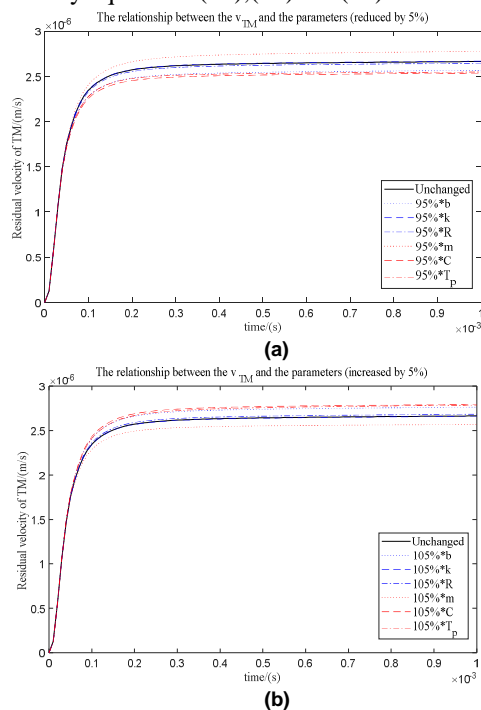


FIGURE 10. The influence of parameter changes on residual velocity . (a) increased by 5%.(b) reduced by 5%.

In order to further explore the relationship between the six parameter values and the residual speed to guide the design of GPRM. By changing the value of each parameter (change by 5%) to calculate the corresponding residual speed of the TM, the relationship diagram shown in Fig. 10 can be obtained. It can be seen that except for the piezoelectric transducer ratio T_p , when the other five parameters decrease, the residual velocity decreases accordingly. The composite stiffness k and circuit resistance R have the greatest influence on the residual velocity of TM. Compared with the composite stiffness k , the circuit resistance R is easier to adjust. Therefore, adjusting the resistance R within the allowable range can more effectively reduce the residual speed of TM to meet the release condition. However, in actual work, how to specifically change the equivalent parameters of the system is still a problem that needs to be studied, and we will carry out this work in the future.

IV. CONCLUSION

Based on the influence of GPRM parameters on TM residual velocity, this paper conducts theoretical research

and simulation analysis, uses adhesion force to link RT displacement and TM residual velocity together, so as to calculate the numerical solution of TM residual velocity. The correspondence between the parameters provides an effective guide plan for the development of GPRM. Aiming at the problem of GPRM parameter identification, this paper proposes an improved cuckoo search algorithm based on population entropy and boundary search strategy. From the results of simulation experiments, it can be seen that under the same number of iterations, the improved algorithm parameter identification success rate and optimization accuracy have been significantly improved, although it is accompanied by a certain degree of calculation increase. Most of the assumptions and constraints of the theory and simulation experiment in this article are based on the reference [3]. In the future, we will build the experimental environment to further study the effectiveness of the method proposed in this paper under actual working conditions.

REFERENCES

- [1] B. P. Abbott, C. Gianpietro, J. Degallaix, V. Dolique, R. Flaminio, M. Granata, et al., "Observation of Gravitational Waves from a Binary Black Hole Merger," *Phys Rev Lett*, vol. 116, no. 6, pp. 061102.1-061102.16, Feb. 2016.
- [2] Vitale S, Bender P, Brillet A, et al. "LISA and its in-flight test precursor SMART-2," *Nuclear Physics B*, vol.110,no.2,pp.209-216, 2012.
- [3] D Bortoluzzi, Conklin J W, Zanoni C. "Prediction of the LISA-Pathfinder release mechanism in-flight performance," *Advances in Space Research*, vol.51, no.7, pp.1145-1156, 2013.
- [4] Bortoluzzi D, MaUsli P A, Antonello R, et al. "Modeling and identification of an electro-mechanical system: The LISA grabbing positioning and release mechanism case," *Advances in Space Research*, vol.47, no.3, pp.457-465, 2011.
- [5] X.-S. Yang and S. Deb, "Engineering optimisation by cuckoo search," *Int.J. Math. Model. Numer. Optim.*, vol. 1, no. 4, pp. 330–343, 2010.
- [6] X.-S. Yang and S. Deb, "Cuckoo search via L vvy flights," in *Proc. World Congr. Nature Biol. Inspired Comput. (NaBIC)*, Coimbatore, India, Dec. 2010, pp. 210–214.
- [7] M. Jiang, J. Luo, D. Jiang, J. Xiong, H. Song, and J. Shen, "A cuckoo search-support vector machine model for predicting dynamic measurement errors of sensors," *IEEE Access*, vol. 4, pp. 5030–5037, Aug. 2016.
- [8] W. Han et al., "Cuckoo search and particle filter-based inverting approach to estimating defects via magnetic flux leakage signals," *IEEE Trans. Magn.*, vol. 52, no. 4, Apr. 2016, Art. no. 6200511.
- [9] J. Wei and Y. Yu, "An effective hybrid cuckoo search algorithm for unknown parameters and time delays estimation of chaotic systems," *IEEE Access*, vol. 6, pp. 6560–6571, Aug. 2018.
- [10] Li Dequan, Xu S, Qi X, et al. "Variable step size adaptive cuckoo search optimization algorithm for phase diversity," *Applied Optics*, vol. 57, no. 28, pp. 8212-8219, Oct. 2018.
- [11] Bortoluzzi, D., Baglivo, L., Benedetti, M., F Biral, Bosetti, P., & Cavalleri, A., et al. "Lisa pathfinder test mass injection in geodesic motion: status of the on-ground testing," *Classical & Quantum Gravity*, vol. 26, no. 9, pp. 094011.1-094011.11, 2009.
- [12] Neukom, A., R. Romano, and P. M. Nellen. "TESTING AND LESSONS LEARNT OF LISA GPRM," in *Proc.13th European Space Mechanisms and Tribology Symposium-ESMATS 2009*, Vienna, Austria, 2009.
- [13] Pierre-Alain M usl, Andreas Neukom, Romeo Romano, Ingo K oker, Steve Durrant. "Development of a Novel Piezo Actuated Release Mechanism," in *Proc.12th Euro. Space Mechanisms & Tribology Symp. (ESMATS)*, Liverpool, UK. 2007.

- [14] Schmid, M., Wernlein, G., & I Köker. "ALTERNATIVE DESIGN APPROACH FOR THE LISA LTP LOCKING ASSEMBLY," in *Proc.14th European Space Mechanisms & Tribology Symposium – ESMATS 2011*, Constance, Germany, 2011.
- [15] Koker, I., Rozemeijer, H., F Stary, & Reichenberger, K. "Alignment and Testing of the GPRM as Part of the LTP Caging Mechanism," in *Proc. 15th European Space Mechanisms & Tribology Symposium – ESMATS 2013*, Noordwijk, The Netherlands, 2013.
- [16] Zahnd B, Zimmermann M, R Spöri. "LISA PATHFINDER CAGE AND VENT MECHANISM- DEVELOPMENT AND QUALIFICATION," in *Proc.15th European Space Mechanisms & Tribology Symposium – ESMATS 2013*, Noordwijk, the Netherlands, 2013.
- [17] D Bortoluzzi, Zanon C, Vitale S. "Improvements in the measurement of metallic adhesion dynamics," *Mechanical Systems & Signal Processing*, vol. 52-53, pp. 600-613, Feb.2015.
- [18] Zanon C, Bortoluzzi D, Conklin J W, et al. "Testing the injection of the LISA-Pathfinder Test Mass into geodesic conditions," Presented at 15th European Space Mechanisms and Tribology Symposium. Available: <https://www.researchgate.net/publication/262105382>
- [19] D Bortoluzzi, Armano M, Caleno M, et al. "Injection of a Body into a Geodesic: Lessons Learnt from the LISA Pathfinder Case," in *Proc.the 43rd Aerospace Mechanisms Symposium*, NASA Ames Research Center, 2016.
- [20] Zanon C , Bortoluzzi D , Conklin J W , et al. "Summary of the results of the LISA-Pathfinder Test Mass release. ," in *Proc. 10th International LISA Symposium*, Florida,USA,2014.
- [21] B. Cao *et al.* "Distributed parallel particle swarm optimization for multiobjective and many-objective large-scale optimization," *IEEE Access*, vol. 5, pp. 8214–8221, 2017.
- [22] S. Bououden, M. H. R. Chadli, and Karimi, "An ant colony optimization based fuzzy predictive control approach for nonlinear processes," *Inf. Sci.*, vol. 299, pp. 143–158, Apr. 2015.
- [23] W. Zhang *et al.*, "An improved ant colony algorithm for path planning in one scenic area with many spots," *IEEE Access*, vol. 5, pp. 13260–13269, 2017.
- [24] J. Zhao, S. Liu, M. Zhou, X. Guo and L. Qi, "An Improved Binary Cuckoo Search Algorithm for Solving Unit Commitment Problems: Methodological Description," in *IEEE Access*, vol. 6, pp. 43535-43545, 2018, doi: 10.1109/ACCESS.2018.2861319.
- [25] Sanchez Giraldo L G , Rao M , Principe J C . "Measures of Entropy from Data Using Infinitely Divisible Kernels ,", *IEEE Transactions on Information Theory*, vol.61, no.1, pp.535-548, 2014.
- [26] S. Zhang, J. Pu and Y. Si, "An Adaptive Improved Ant Colony System Based on Population Information Entropy for Path Planning of Mobile Robot," in *IEEE Access*, vol. 9, pp. 24933-24945, 2021, doi: 10.1109/ACCESS.2021.3056651.



DONG WANG was born in Shanxi, China. He received the Ph.D. degree from the University of Chinese Academy of Sciences, Beijing. He is currently an professor of space optics department, changchun institute of optics, fine mechanics and physics, chinese academy of sciences. He is currently the Vice-Director of the space optics research department III, CIOMP, CAS. His research interests include precision displacement control and image processing.



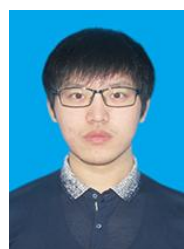
ZHI WANG received the B.S. and M.S. degrees in mechanical engineering from the Changchun University of Science and Technology, in 1985 and 1988, respectively, and the Ph.D. degree in optical engineering from CIOMP, in 1998. He is currently the Vice-Director of the space optics research department I, CIOMP, CAS. His research interest includes design and manufacturing of space telescope and interferometric systems.



XINGGUO SUN was born in Jilin, China. He received the B.S. and M.S. degree from the Jilin University, Changchun. He is currently an senior engineer of FAW-Volkswagen Automobile Co., Ltd. His research interests include precision automatic control and high precision machining.



DEQUAN LI was born in Liaoning, China. He received the Ph.D. degree from the University of Chinese Academy of Sciences, Beijing. He is currently an assistant researcher of space optics department, Changchun institute of optics, fine mechanics and physics, Chinese academy of sciences. His research interests include precision displacement control, gravitational reference sensor development, active optics, deep learning and deep reinforcement learning.



HONGDA LIU was born in Heilong Jiang, China. He received the B.S. degree from the Harbin Institute of Technology. He is currently pursuing the master's degree from university of Chinese Academy of Sciences. His research interests include intelligent optimization algorithms, and precision displacement control.